ified conditions, cm.

h = total length of column, cm.

J = rate of interphase mass transfer of CNB, g./sec.

K = coefficient of mass transfer between solid and liquid phases, cm./sec.

L = mass flow of solid, g./sec.

m = slope of phase relation (4), dimensionless

N = diffusional flow of material, g./sec.

q = constant in general solution to differential equation, defined by characteristic equation, $cm.^{-1}$

R = constant defined by Equations (5)

V = mass flow of liquid, g./sec.

X = weight fraction CNB or cyclohexane in solid, g./g.

Y = weight fraction CNB or cyclohexane in liquid, g./g.

z = position in the column, measured from freezing section, cm.

α = ratio of adhering liquid to crystal

Δ = small increment

η = volume fraction, dimensionless

ρ = density, g./cc.

Subscripts

C = CNB

0 = position, $z = 0$

1, 2 = position in column

Superscripts

* = equilibrium value

$'$ = model describing eutectics

LITERATURE CITED

1. Albertins, R., Ph.D. dissertation, Univ. Mich., Ann Arbor (1967).
2. ———, W. C. Gates, and J. E. Powers, in "Fractional Solidification," M. Zief and W. R. Wilcox, ed., Marcel Dekker, New York (1967).
3. Albertins, R., and J. E. Powers, *AIChE J.*, **15**, 554 (1969).
4. Anikin, A. G., *Dokl. Akad. Nauk SSSR*, **151**, No. 5, 1139 (1963).
5. ———, *Russ. J. Phys. Chem.*, **37**, No. 3, 377 (1963).
6. Furry, W. H., R. C. Jones, and L. Onsager, *Phys. Rev.*, **55**, 1083 (1939).
7. Gates, W. C., Ph.D. dissertation, Univ. Mich., Ann Arbor (1967).
8. Jones, S. C., Ph.D. dissertation, Univ. Mich., Ann Arbor (1962).
9. Lewis, J. B., *Chem. Eng. Sci.*, **3**, 248 (1954).
10. Moon, J. S., Ph.D. dissertation, Univ. Calif., Berkeley (1964).
11. Powers, J. E, in "Symposium uber Zonenschmelzen und Kolonnen Kristallisieren," H. Schildknecht, ed., p. 57, Kernforschungszentrum, Karlsruhe, Germany (1963).
12. Roessler, S., Ph.D. dissertation, Univ. Erlangen, Germany (1961).
13. Schildknecht, H., Paper presented at 56 National Meeting, Am. Inst. Chem. Engrs., San Francisco, Calif. (1965).
14. ———, *Anal. Chem.*, **181**, 254 (1961).
15. Smoot, L. D., and A. L. Babb, *Ind. Eng. Chem. Fundamentals*, **1**, 93 (1962).
16. Thorsen, G., and S. G. Terjesen, *Chem. Eng. Sci.*, **17**, 137 (1962).
17. Yagi, S., H. Inove, and H. Sakamoto, *Kagaku Kogaku*, **27**, No. 6, 415 (1963).
18. Henry, J. D., Jr., and J. E. Powers, *AIChE J.*, to be published.

Manuscript received April 22, 1968; revision received November 13, 1968; paper accepted November 14, 1968.

Experimental and Computational Studies of the Dynamics of a Fixed Bed Chemical Reactor

JOSÉ SINAI and A. S. FOSS

University of California, Berkeley, California

Experimental measurements of the temperature response of a fixed bed reactor to sinusoidal disturbances in the feed concentration, temperature, and flow rate show that a simple one-dimensional mathematical model with distributed thermal capacitance satisfactorily describes the dynamic behavior of the reactor for modest excursions about an operating point. The reaction considered is a liquid-phase exothermic reaction whose rate depends on the concentration of two reactants and the temperature.

A computational analysis reveals that the amplitude and phase of the traveling concentration and temperature waves are influenced in a complex manner by the interaction between the two waves. The interaction, which is treated here as interference between traveling waves, is made complex by the difference in the rates of propagation of the temperature and concentration waves and by the variation of their speeds throughout the bed.

Concentration and temperature disturbances are known to propagate through fixed bed chemical reactors in a wavelike manner. While knowledge of the interactions between these traveling waves is central to the conception and design of reactor control systems and to the design of the reactors themselves, there has been only limited exploration of the nature of such phenomena. This paper reports computational and experimental studies of the interaction of traveling sinusoidal concentration and temperature disturbances originating in the reactor feed.

José Sinai is currently with Esso Mathematics & Systems, Inc., Florham Park, New Jersey.

The interaction between traveling concentration and temperature disturbances is particularly interesting in fixed bed reactors because the propagation speed of the temperature wave differs from the speed of the concentration wave (*13*). In the absence of packing, both waves would travel at the fluid velocity. Owing to the thermal capacity of the packing, however, the temperature wave travels slower than the fluid. The ratio of the temperature wave velocity to the fluid velocity is equal to the fraction of the total heat capacitance of the system contributed by the fluid (*3*). Thus, for liquid reactants, the velocity of the temperature wave is about one half the fluid velocity and for gaseous reactants, about one thousandth. Concentration waves, on the other hand, travel at yet some other velocity which depends on the adsorptive capacity of the packing for the components in the fluid. In many instances, the adsorptive capacity is negligible, in which case the concentration wave tends to travel at the fluid velocity, but it is not entirely free to do so owing to its coupling with the temperature wave. Thus, since the propagation velocity of temperature and concentration waves are generally different, a phase difference exists between the waves as they propagate through the bed. This phase difference varies from one location to another, depending both on the rate of the transfer processes and on the rate of chemical reaction. At some locations within the bed, one finds that owing to the particular phase difference between the temperature and the concentration waves, these waves may act in concert to enhance the reaction rate disturbance. On the other hand, at other reactor locations, the phase difference may cause the waves to have opposing effects on that rate. Such a phenomenon is likened here to the interference phenomenon in traveling wave trains. Temperature and concentration waves acting in accord or discord with respect to their influence on the reaction rate are analogous to the constructive and destructive interference phenomena.

Interacting concentration and temperature waves are studied here for a packed reactor in which the homogeneous exothermic reaction between aqueous solutions of sodium thiosulfate and hydrogen peroxide occurs. The stoichiometry of this reaction, as determined by Spencer (*11*), is represented by

$$Na_2S_2O_3 + \gamma H_2O_2 \rightarrow \text{products}$$

and the rate of reaction, also determined by Spencer, is

$$\text{rate} = k\, e^{-E/RT^*} A^* \cdot B^*$$

The packing, which consisted of glass spheres, was chemically inert and was placed in the reactor for the express purpose of retarding the propagation velocity of the temperature wave.

Because the rate of reaction is a nonlinear function of temperature and concentration, interaction between traveling disturbances is, in general, of a nonlinear nature. Some interesting stability phenomena that arise as a result of this nonlinear interaction have been studied by Liu and Amundson (*5*) and by McGuire and Lapidus (*6*). The attention of this investigation, however, is directed to the study of disturbances deviating only slightly about a steady state. A change in the local rate of reaction can then be treated as a linear function of temperature and concentration deviations. It is important, however, that the nonlinear nature of the process be retained in establishing the steady state about which excursions occur. Disturbances, therefore, may be viewed as behaving linearly in a reactor in which the reaction rate sensitivity with respect to temperature and concentration is a nonuniform function of position. One of the objectives of this investigation was to elucidate the influence of the nonuniformity of reaction rate sensitivity on the propagation of interacting traveling waves of concentration and temperature.

A second objective of this work was to verify that the principal effects governing disturbance propagation in fixed bed reactors are, indeed, the nonuniformity of reaction rate sensitivity to concentration and temperature along the bed and the dispersion effects originating from finite rates of heat transfer between fluid and packing. This verification was accomplished by comparing experimentally determined frequency response characteristics with the predictions of a mathematical model of the reactor which included only the above effects. The reactor was represented by a one-dimensional differential model with no axial fluid mixing. The small sinusoidal deviations of temperature and concentration about a steady state were treated by a linear perturbation analysis. In this respect, this work resembles the studies of Tinkler and Lamb (*12*).

The computational studies presented here emphasize disturbance propagation phenomena as distinguished from the determination of transfer function relationships for the reactor. The former includes the latter and further, provides physical insight which is not so easily derived from the transfer functions alone. It is anticipated that knowledge of the phenomenon of interference between traveling concentration and temperature waves can be exploited in the search for new methods of reactor control.

FORMULATION OF THE MATHEMATICAL MODEL

Numerous studies of packed bed processes under both transient and steady state conditions have shown the accuracy of mathematical models which treat the bed as a continuum and which ignore its particulate nature. The model used in this work is a continuum representation; in it are embodied the assumptions of finite fluid-particle thermal resistance, plug flow, and the absence of axial mixing. The dimensionless differential mass and heat balances which comprise this model are

Mass balance for reactant A:

$$\frac{\partial A}{\partial \tau} + V\frac{\partial A}{\partial z} = -r = -KAB\exp\{\mathfrak{A}T/(T_o + T)\} \quad (1)$$

Mass balance for reactant B:

$$\frac{\partial B}{\partial \tau} + V\frac{\partial B}{\partial z} = -\gamma \cdot r \quad (2)$$

Heat balance for fluid:

$$\frac{\partial T}{\partial \tau} + V\frac{\partial T}{\partial z} = r - H_w(T - T_w) - H_p(T - T_p) \quad (3)$$

Heat balance for packing:

$$\frac{\partial T_p}{\partial \tau} = H_p\beta_p(T - T_p) \quad (4)$$

Heat balance for reactor wall:

$$\frac{\partial T_w}{\partial \tau} = H_w\beta_w(T - T_w) + H_e\beta_w(T_e - T_w) \quad (5)$$

where the dimensionless parameters are

$$K \equiv kA_r\frac{L}{V_r}\exp(-\mathfrak{A}) \quad (6)$$

$$H_p \equiv \frac{h_p a_p L}{\epsilon V_r \rho_f c_f} \quad (7)$$

$$\beta_p \equiv \frac{\epsilon \rho_f c_f}{(1-\epsilon)\rho_p c_p} \tag{8}$$

Definitions of the parameters H_e, H_w, and β_w are analogous. In the above equations, temperatures have been normalized with respect to the adiabatic temperature rise and concentrations normalized with respect to the steady state concentration of limiting reactant (reactant A) in the feed. Combination of Equations (1) and (3) shows that the following relation holds for adiabatic reactors at steady state:

$$T_s(z) + A_s(z) = 1$$

This relationship states in simple form the well-known equivalence of conversion and temperature change in adiabatic reactors.

In formulating the model, the fluid is considered incompressible, and its density and heat capacity are assumed independent of fluid temperature and concentration; this approximation is valid for liquids but is not generally valid for gases.

Among the several assumptions incorporated in this formulation, perhaps that of plug flow (implying the radial uniformity of fluid velocity) is most often open to question. Numerous studies by others, which have detected appreciable deviations from uniformity, show that the deviations for gases are usually larger than those for liquids. Measurements of Cairns and Prausnitz (*1*) with water showed an insignificant radial variation of velocity when the ratio of tube to particle diameter was 16, while those of Schwartz and Smith (*10*) with air showed velocity deviations as large as 40% when the ratio was 10. For the case of liquid reactants considered here, the radial uniformity of velocity appears to be an adequate assumption. Thus, for a reactor of constant cross section, this assumption and those above imply a uniform fluid velocity radially and axially under all dynamic and steady state conditions.

A closely related assumption is that of radially uniform temperature. For the particular reaction system under consideration, calculations (*3*) have shown that owing to the high effective radial thermal conductivity of the bed, radial temperature gradients are quite small and have an insignificant influence on the dynamic behavior of the reactor.

The justification for neglecting axial fluid mixing (and axial heat conduction) seems well established by prior studies. An analysis by Petersen (9) shows that the effect of axial fluid dispersion is rarely an important consideration in tubular reactors. Moreover, an earlier computational study (3) has found that the effect of fluid mixing on the transient response of a packed tubular reactor is far overshadowed by the dispersion of heat due to the finite rate of fluid-particle heat transfer.

Finally, the influence of the thermal resistance within the packing particles has also been neglected here because that influence is known to be small. For the conditions prevailing in the experiments reported here, calculations based on the results of Meek (7) indicate a negligible influence of finite conduction rates within the particle and the tube wall.

Among the number of parameters associated with the above model, the significance of three is mentioned here. The parameter H_p is the number of transfer units for fluid-particle heat transfer, and its reciprocal may be interpreted as the time constant for fluid temperature response. The parameter β_p is the fluid-particle heat capacitance ratio. The quantity $1/H_p\beta_p$ is the thermal time constant for a particle. Since β_p is of order unity for liquid reactants, the two time constants have essentially the same value. As has been long recognized, the parameter $\mathfrak{A} \equiv E/RT_r$ is a measure of the interaction between concentration and temperature. The influence of this parameter on dynamic response is exerted fully in adiabatic reactors but not at all in isothermal reactors.

APPROXIMATE MODEL FOR SMALL DISTURBANCES

Interest in this work has centered on the solution of the above equations when concentration and temperature make only small sinusoidal excursions about their steady state values. For such purposes, a local linearization of Equations (1) through (5) about a steady state is made, and the following equations are obtained:

$$\frac{\partial a}{\partial \tau} + \frac{\partial a}{\partial z} = -r_A a - r_B b - r_T t + r_s v \tag{9}$$

$$\frac{\partial b}{\partial \tau} + \frac{\partial b}{\partial z} = \gamma\,(-r_A a - r_B b - r_T t + r_s v) \tag{10}$$

$$\frac{\partial t}{\partial \tau} + \frac{\partial t}{\partial z} = r_A a + r_B b + r_T t - H_p(t - t_p) - H_w(t - t_w) - T_s' v \tag{11}$$

$$\frac{\partial t_p}{\partial \tau} = H_p \beta_p (t - t_p) \tag{12}$$

$$\frac{\partial t_w}{\partial \tau} = H_w \beta_w (t - t_w) + H_e \beta_w (t_e - t_w) \tag{13}$$

where

$$\left.\begin{aligned} r_A &\equiv \frac{\partial r_s}{\partial A_s} = r_s/A_s \\ r_B &\equiv \frac{\partial r_s}{\partial B_s} = r_s/B_s \\ r_T &= \frac{\partial r_s}{\partial T_s} = r_s \cdot \frac{\mathfrak{A} T_o}{(T_o + T_s)^2} \end{aligned}\right\} \tag{14}$$

A statement of the boundary conditions and initial conditions for these equations is deferred to a succeeding paragraph.

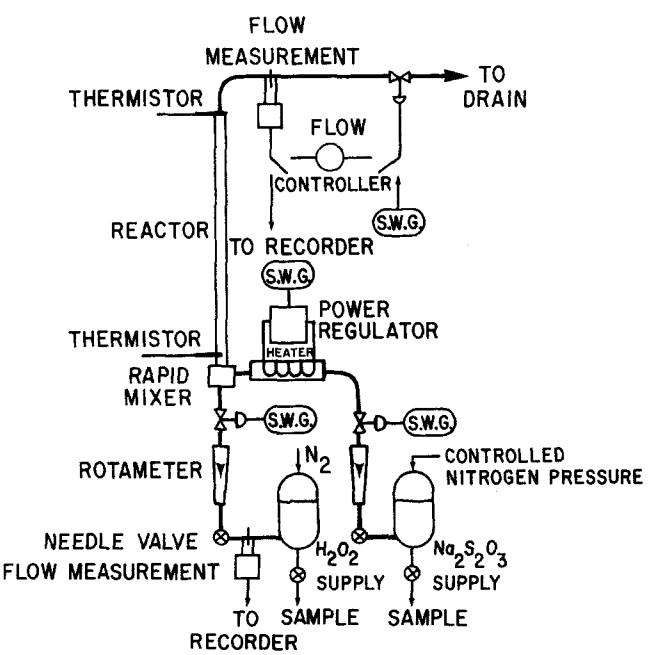

Fig. 1. Flow diagram of experimental system.

$$m \equiv \frac{H\beta}{H_p\beta_p} = \frac{1+NP}{1+\left[1+\left(\frac{\beta_w}{\beta_p}\right)^2 \frac{H_e(H_w+H_e)}{H_p{}^2\omega_1{}^2}\right]P - \frac{H_wH_e}{H_p(H_w+H_e)}\left[1+\frac{1}{\omega_1{}^2}\right]}$$

$$\frac{H}{H_p} = \frac{\omega_1{}^2+m^2}{\omega_1{}^2+1}\left[1+\frac{NP}{m}\right] \qquad (19)$$

where

$$\omega_1 = \frac{\omega}{H_p\beta_p}; \quad N = \frac{H_w\beta_w}{H_p\beta_p};$$

$$P = \frac{H_w}{H_p}\left[\frac{\omega_1{}^2+\left(\frac{\beta_w}{\beta_p}\right)^2\left(\frac{H_w+H_e}{H_p}\right)^2}{\omega_1{}^2+1}\right]$$

The coefficients $r_T(z)$, $r_A(z)$, and $r_B(z)$ represent the local sensitivity of the reaction rate with respect to temperature and concentration of species A and B. The coefficients r_s and T_s' of the v terms represent the local sensitivity of the rate of reactant consumption and heat generation with respect to the average fluid velocity. Velocity variations also affect the heat transfer parameters H_p and H_w, but because this effect is small, it has not been considered. The above coefficients depend only on the steady state about which excursions occur and are calculable from the solutions of the ordinary differential equations that describe it. These equations are

$$\frac{dA_s}{dz} = -r_s = -KA_sB_s \exp\{\hat{n}T_s/(T_o+T_s)\} \qquad (15)$$

$$\frac{dB_s}{dz} = -\gamma r_s \qquad (16)$$

$$\frac{dT_s}{dz} = r_s - U(T_s - T_e) \qquad (17)$$

The boundary conditions for these equations are

$$A_s(0) = 1; \quad B_s(0) = B_s{}^*(0)/A_r; \quad T_s(0) = 0 \qquad (18)$$

A SIMPLIFICATION OF THE MODEL

It is possible to effect a simplification of the linear model, Equations (9) to (13), which offers some reduction in the complexity of the description of the heat transfer processes. The proposal is to consolidate into a single term the expression for the rate of accumulation of heat in both the particles and the reactor wall. The heat balance for the wall, Equation (13), is discarded entirely, and heat balances for the fluid and particles, Equations (11) and (12), are modified as follows:

$$\frac{\partial t}{\partial \tau} + \frac{\partial t}{\partial z} = r_Aa + r_Bb + r_Tt - H(t-t_m) - U(t-t_e) - T_s'v \qquad (11a)$$

$$\frac{\partial t_m}{\partial \tau} = H\beta(t-t_m) \qquad (12a)$$

All solid media, which in the above formulation are now indistinguishable, have temperature t_m, thermal capacitance ratio β, and heat transfer parameter H. By consideration of the heat transfer problem alone, the above formulation can be shown to be exact for steady sinusoidal forcing when parameters H and β are assigned values as follows:

Although the above relationships show that H and β should be assigned values depending on frequency, it is normally found that H and β are insensitive to frequencies over the range of interest. The parameters H and β are most sensitive to frequency when the ratio H_w/H_p takes on values very large or very small compared with unity. By contrast, H and β are entirely insensitive to frequency when the ratio β_w/β_p takes on very large or very small values.

When applied to the experimental reactor of this study, the above relations show that H and β may be taken independent of frequency and are given by

$$\frac{1}{\beta} = \frac{1}{\beta_p} + \frac{1}{\beta_w} \qquad (20)$$

$$H = H_p + H_w$$

These relations obtain because the reactor was operated adiabatically ($H_e = 0$), and the time constants for the wall and particles were approximately equal ($N \cong 1$).

CALCULATION OF THE FREQUENCY RESPONSE

The steady sinusoidal response of the model may be determined easily through the Laplace transformation of the equations. Application of the Laplace transformation to Equations (9), (10), (11a), and (12a) gives

$$\frac{d\bar{a}}{dz} = -(r_A+s)\bar{a} - r_B\bar{b} - r_T\bar{t} + r_s\bar{v} \qquad (21)$$

$$\frac{d\bar{b}}{dz} = \gamma[-r_A\bar{a} - (r_B+s)\bar{b} - r_T\bar{t} + r_s\bar{v}] \qquad (22)$$

$$\frac{d\bar{t}}{dz} = r_A\bar{a} + r_B\bar{b} + \left\{r_T - s - \frac{Hs}{s+H\beta} - U\right\}\bar{t} + U\bar{t}_e - T_s'\bar{v} \qquad (23)$$

The initial conditions have been taken as zero because they are of no importance in the determination of the steady sinusoidal response. Since a general solution to these equations is not known except for the special case of an adiabatic reactor with a single first-order reaction (4), they were solved numerically. The functions r_A, r_B, etc., were determined by simultaneous solution of the steady state Equations (15) through (18). A fourth-order Runga-Kutta method was used. The amplitude and phase of the variables a, b, and t are determined, as is well known, by calculation of the magnitude and angle of the complex variables $\bar{a}$, $\bar{b}$, and $\bar{t}$. In these calculations, the

complex variable s is replaced by the pure imaginary quantity $(i\omega)$. For the forcing of each variable separately, the boundary conditions $\bar{a}\ (s, 0)$, $\bar{b}\ (s, 0)$, and $\bar{t}\ (s, 0)$ may be taken simply as unity (real) for the forced variable and zero for the variables held constant; the forcing of the fluid velocity is treated similarly. The simultaneous forcing of two or more variables having any desired relative amplitude and phase relationships among them may be achieved by assigning appropriate complex-valued boundary conditions.

EXPERIMENTAL REACTOR SYSTEM

The schematic flow diagram of the experimental reactor system is shown in Figure 1. The reactor was constructed from a 1-in. O.D. stainless steel tube of 0.010-in. wall thickness. The tube was positioned vertically and was randomly packed with 3-mm. borosilicate glass spheres, the length of the packed section being 100 cm. A dead air space between the reactor and a concentric outside tube served as a heat insulator. The reactant solutions were fed to the reactor through a rapid premixing device of the Hartridge-Roughton type in which rapid and intimate mixing of both species were achieved before any appreciable reaction occurred. The time spent by the solutions in the mixing cavity and the connecting passage to the reactor was less than 0.1 sec.; the residence time in the reactor proper was 13.4 sec. Measurements of the temperature of reactants entering and leaving the mixer confirmed that the extent of reaction prior to its entrance into the packed section was negligible. Table 1 summarizes the parameters for the reactor. Since the specific heats of the packing and the wall were not measured, the thermal capacities cited in Table 1 should be considered approximate.

Temperature variations in the reactant feed stream were produced by sinusoidal electric heating of the sodium thiosulfate solution just before it entered the premixing device. Sinusoidal flow rate variations were produced by means of a pneumatic flow control valve located downstream from the reactor. The variations of concentrations were produced by simultaneous variation of the flow rates of both reactants via the flow control valves shown in the reactant lines. These sinusoids in reactant flow rates were of equal magnitude and out of phase by 180 deg., so that the total flow rate remained constant. A flow control device located in the reactor effluent stream assured constancy of the total flow. In all these experiments, sinusoids were obtained from an electronic sine-wave generator. The periods of the sinusoids ranged from about 70 to 8 sec. The temperature of the surroundings was not treated as a forcing variable in these experiments. Nor was the surroundings temperature considered a parameter because the reactor tube was essentially adiabatic.

Table 1. Reactor Physical Parameters

Tube diameter, I.D.	0.980 in.
Tube wall thickness	0.010 in.
Length of packed section	100 cm.
Tube material	Stainless steel, type 304
Tube thermal capacitance	19.5 cal./°C. [based on a density of 8 g./cc. and a specific heat of 0.12 cal./(g.)(°C.)]
Tube wall thermal conductivity	10 B.t.u./(hr.)(ft.)(°F.)
Packing particle diameter	3 mm.
Packing material	Borosilicate glass
Packing thermal capacitance	142.3 cal./°C. [based on a specific heat of 0.20 cal./(g.)(°C.)]
Packing thermal conductivity	0.6 B.t.u./(hr.)(ft.)(°F.)
Packing void fraction	0.416

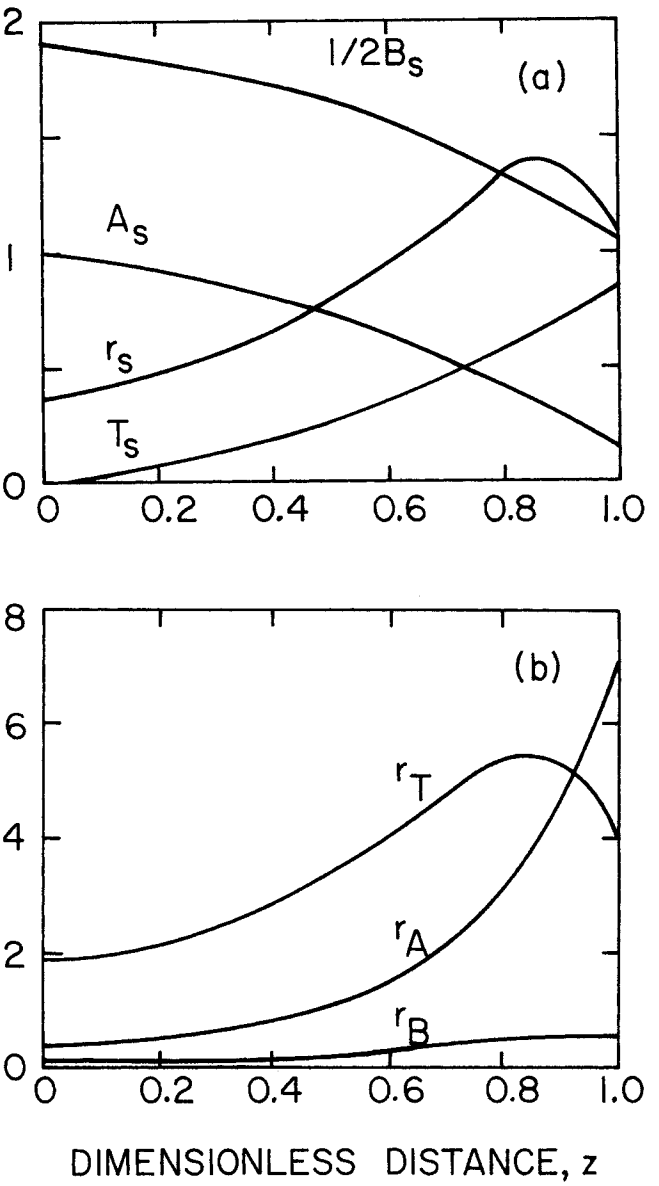

Fig. 2. Reactor variables and sensitivity functions at steady state: conditions of column 2, Table 2.

During the introduction of the sinusoids, continuous measurement and recording of fluid temperature were made with small thermistors placed at both ends of the packed section. When necessary, flow rates were continuously measured and recorded. Sinusoidal concentration variations at the reactor inlet were determined from continuous flow rate measurements. The concentration of the reactants in the reservoirs was determined by chemical methods.

An auxiliary experiment was performed to determine values of the parameters H and β of Equations (11a) and (12a). Water was fed to the packed tube, and the effluent temperature was measured for sinusoidal forcing of the temperature of the influent stream. Expressions relating the amplitude and phase to H, β, and frequency in this simple heat exchange process can be determined by solution of Equations (11a) and (12a) with $r_T = r_A = r_B = U = 0$ and $t(\tau, 0) = \sin \omega\tau$. These relations are

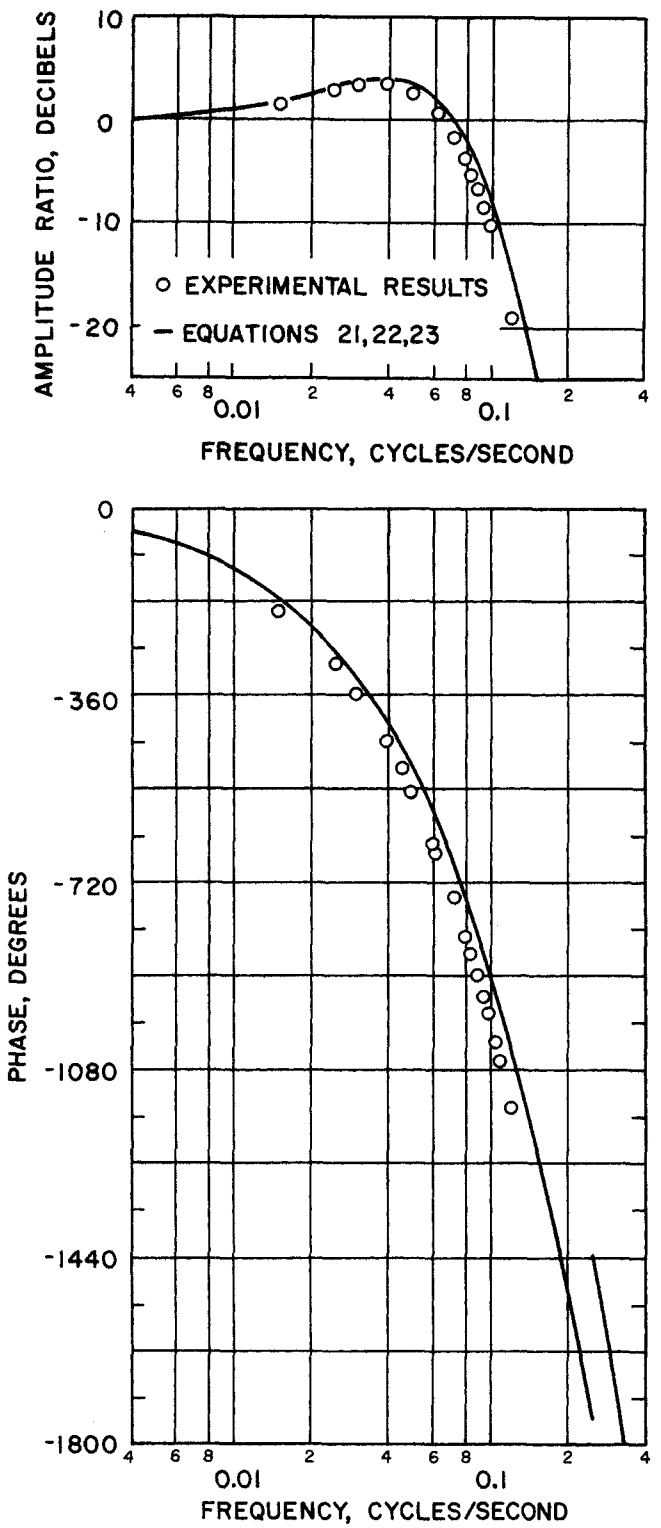

Fig. 3. Comparison of experimental and computed frequency response: response of effluent temperature to feed temperature variation.

$$\text{Amplitude} = M_T = \exp\left\{ -\frac{H\omega^2}{(H\beta)^2 + \omega^2} z \right\} \quad (24)$$

$$\text{Phase} = \varphi_T = -\omega z \left(1 + \frac{H^2\beta}{(H\beta)^2 + \omega^2} \right) \quad (25)$$

At low frequencies ($\omega << H\beta$), it is seen that for $z = 1$

$$M_T \cong \exp\left\{ -\frac{\omega^2}{H\beta^2} \right\} \quad (24a)$$

$$\varphi_T \cong -\left(1 + \frac{1}{\beta} \right) \omega \quad (25a)$$

The values of H and β given in Table 2 were determined from the straight-line graphs of φ_T vs. ω and log M_T vs. ω^2. For the conditions of the reactor experiments, the value of the combined fluid-solid heat transfer coefficient h was 182 B.t.u./(hr.)(sq.ft.)(°F); values of the individual coefficients h_p and h_w could not be determined from this single experiment.

The steady state conditions of the experiments were chosen such that about 90% of the thiosulfate reacted in the packed section. The temperature rise corresponding to this conversion was about 38°C., and measurement of this temperature rise agreed within 1.2% with calculations based on the reaction parameters reported by Spencer (*11*). A summary of the operating conditions for the experiments reported here is given in Table 2. Typical concentration, temperature, and reaction rate profiles obtaining under conditions of the experiments are plotted in Figure 2*a*. The sensitivity functions r_T, r_A, and r_B at the same steady state are shown in Figure 2*b*. The sensitivity functions show that the first 92% of the reactor is more sensitive to temperature disturbances than to concentration disturbances, and that the reverse obtains in the latter 8%. Had stoichiometric amounts of reactants been fed, however, the r_A function in the latter 8% of the reactor would be comparable in magnitude to r_T and would decrease with reactor length in a manner similar to the r_T function.

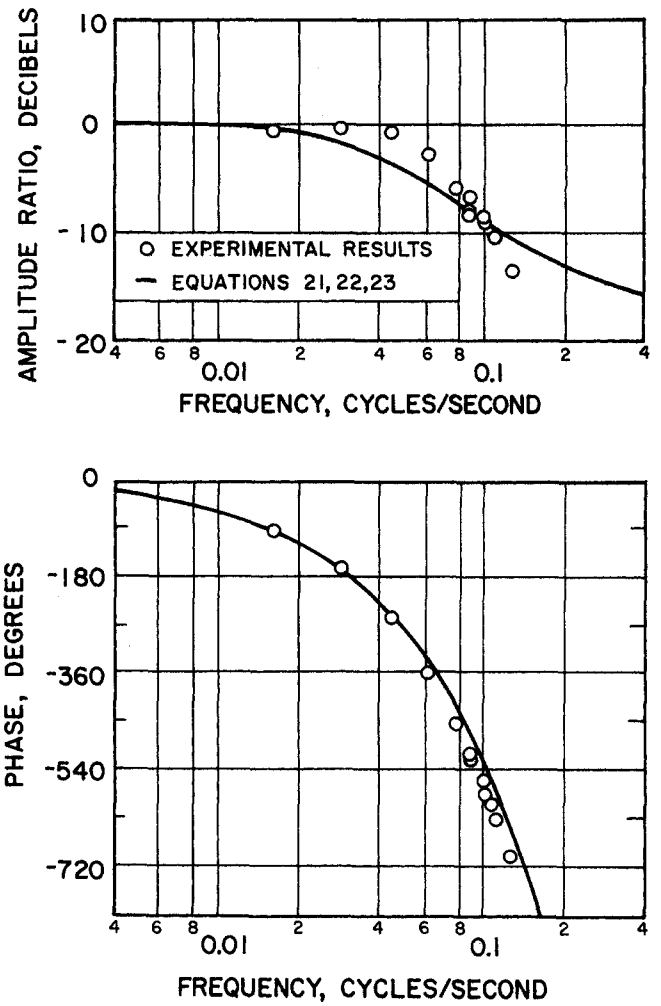

Fig. 4. Comparison of experimental and computed frequency response: response of effluent temperature to the simultaneous variation of the feed concentration of both reactants.

EXPERIMENTAL RESULTS AND COMPARISON WITH MODEL

The experimental and calculated amplitude ratio and phase of the effluent temperature responses as a function of frequency are shown in Figures 3 to 5 for the three types of forcing considered. The amplitude ratio is normalized by the steady state gain and is expressed in decibels. These results are presented for the purpose of introducing some of the interesting features of the frequency response of the reactor and of displaying comparisons between computed and experimentally determined dynamic characteristics.

An interesting phenomenon shown in Figures 3 and 5 is the occurrence of discontinuities in the phase which sometimes may be accompanied by minima and maxima in the amplitude ratio. This behavior is characteristic of multivariable processes with parameters distributed nonuniformly and is a consequence of the manner in which disturbances interfere as they propagate through the reactor. These interference effects are discussed below.

For the case of flow forcing, resonance occurs at high frequencies as shown in Figure 5 by the oscillatory behavior of the phase angle about a limiting value together with minima and maxima in the amplitude ratio. This behavior of distributed parameter systems always results when the forced variable is not a dependent variable. Cohen and Johnson (2) give a detailed analysis of this phenomenon for a steam-liquid heat exchanger. For the chemical reactor, the analysis is complicated by interaction among dependent variables. At high frequencies, however, the interactions become small, and an approximate analysis that decouples concentration and temperature effects predicts that the temperature phase should oscillate about −270 deg. The numerical results displayed in Figure 5 predict a limiting phase of −250 deg. for the temperature response. A corresponding analysis for the effluent concentration response shows the limiting phase angle to be −90 deg. These high frequency characteristics, however, are of little practical importance because the model is no longer valid at these frequencies.

The agreement shown here between experimental and calculated results is considered good, especially in the case of velocity forcing, and indicates that the first-order model considered here adequately accounts for the principal phenomena. A significant result is that the linearized model represents the process well, in spite of the slight distortion of the sinusoid that was observed in some instances. Distortion was observed during velocity forcing at low frequency. There, the sinusoid became slightly skew, resembling the response of a flow-forced heat exchanger (8). The skewness was undetectable at moderate and high frequencies, however. Upon increasing the amplitude of the velocity from 10 to 25%, significant depressions were observed in the crests of the measured temperature response. No study was made of this behavior; all the results presented here were observed by using a velocity-forcing amplitude of 10%. On the other hand, for the forcing of either the feed concentration or feed temperature, no significant distortion was observed, even though relatively large excursions in concentration and temperature did occur at points within the reactor. In the case of temperature forcing, for example, it is estimated that the concentration amplitude at the reactor

TABLE 2. SUMMARY OF EXPERIMENTAL CONDITIONS

	Type of forcing		
	Inlet temp.	Inlet conc. of both reactants	Total flow rate
Steady state conditions			
Conc. of feed to packed section, g.-moles/liter			
Thiosulfate	0.301	0.340	0.303
Peroxide	1.419	1.300	1.610
Feed temperature, °C.	24.6	22.9	24.3
Measured temperature rise, °C.	37.4	37.0	39.1
Percent conversion	94.3	82.4	97.7
Dimensionless parameters*			
T_o	7.49	6.60	7.44
β	30.93	31.10	30.96
K	0.1016	0.09672	0.1001
Dynamic conditions			
Amplitude of forcing (% of steady state value)	± 0.336% (± 1°C.)	± 10%	± 10%
Steady state gain			
Temperature response	2.84 °C./°C.	89.3°C./g.-mole/liter	−0.835°C./cm./sec.
Concentration response	−0.0139 g.-mole/liter/°C.	$0.32 \frac{\text{g.-mole/liter}}{\text{g.-mole/liter}}$	$0.0059 \frac{\text{g.-mole/liter}}{\text{cm./sec.}}$

Conditions common to all runs

Total flow rate = 921 ml./min.
Reynolds number, $D_pG/\mu = 150$
Fluid residence time in packed section = 13.41 sec.
Interstitial velocity = 7.5 cm./sec.
$H = 17.0$ $\beta = 1.17$

* Determined by using the following data of Spencer (11):
$k = 0.685 \times 10^{15}$ sec.$^{-1}$ (g.-mole thiosulfate/cc.)$^{-1}$
$E = 18{,}300$ cal. mole^{-1} °K.$^{-1}$
$(-\Delta H) = 132{,}000$ cal. (g.-mole thiosulfate)$^{-1}$
$\gamma = 2$

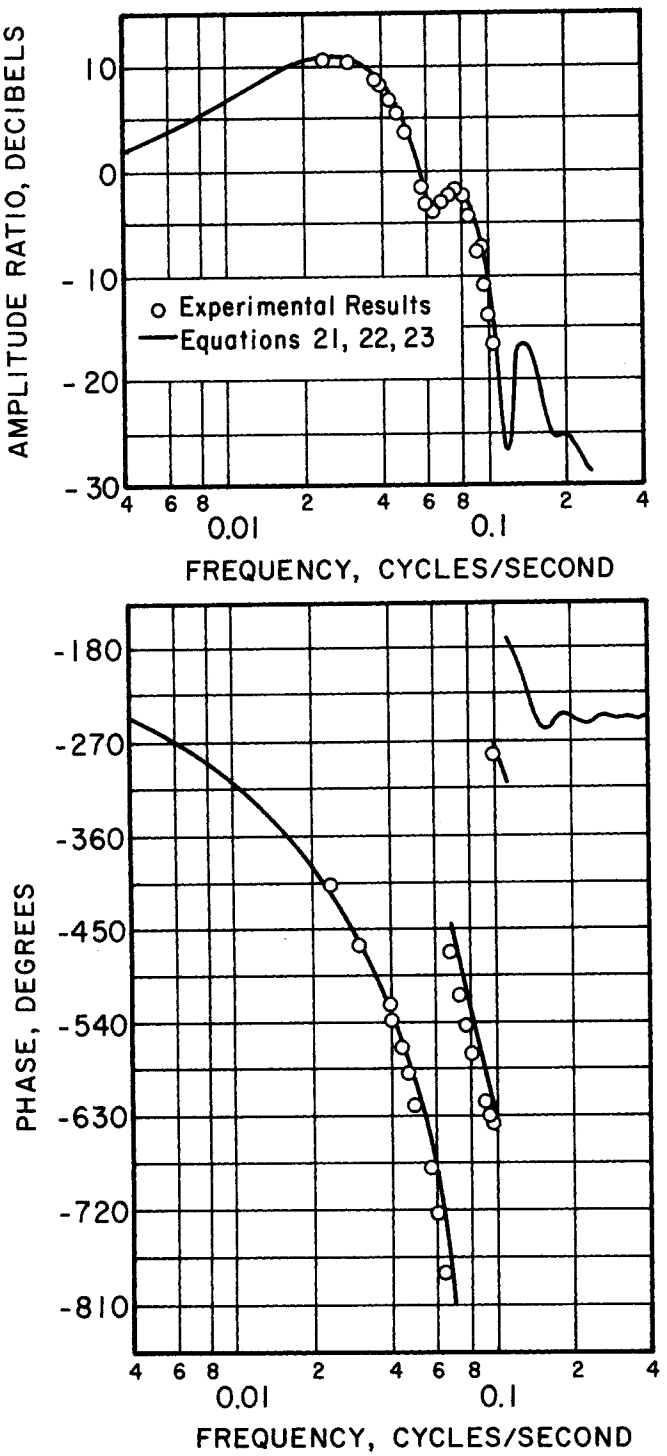

Fig. 5. Comparison of experimental and computed frequency response: response of effluent temperature to flow rate variation.

effluent was 80% of the steady state concentration at that point. That this large deviation in concentration resulted in no appreciable nonlinearity in the measured temperature derives from the dominance of the temperature wave throughout the entire bed. As a further example, temperature excursions of ± 5°C. occurring near the point of maximum reaction rate produced no significant distortion of the measured temperature sinusoid.

INTERPRETATION OF DISTURBANCE PROPAGATION

The importance of the several phenomena that influence the motion of the concentration and temperature waves may be studied through examination of the spatial dependence of the wave amplitude and phase at selected frequencies. These dependencies as calculated from Equations (21) through (23) for both concentration forcing and temperature forcing are shown in Figures 6 and 7 and are discussed below.

Phase Behavior

Concentration Forcing. PHASE OF CONCENTRATION. At low frequencies, the amplitudes graphed in Figure 6 show that the first 50% of the reactor is dominated by concentration disturbances. In this region, the concentration phase behaves nearly as it would were reaction absent, that is, as $\varphi = -\omega z$. The last half of the reactor, however, is dominated by temperature disturbances; the last portion of the reactor may be said, therefore, to be temperature forced. Under such circumstances, the phase relation between the temperature and the concentration must be nearly π (exactly π in an unpacked reactor). Figure 6 shows that the phase of concentration (the nondominant variable) is altered rapidly to satisfy that relation. A phase increase occurs because a phase decrease would require at some point an equivalence of temperature and concentration phase, and this is possible only when the concentration disturbance dominates.

As the frequency increases, Figure 6 shows that the temperature dominance in the last portion of the reactor is overtaken by concentration. For frequencies greater than 7, concentration is clearly dominant everywhere, and as a consequence, the phase of concentration behaves almost as $\varphi = -\omega z$.

PHASE OF TEMPERATURE. In regions of concentration dominance, the chemical reaction tends to align the temperature phase with the concentration phase. The heat transfer between fluid and packing, however, slows the advance of the temperature wave relative to the concentration wave, and hence the phases of the two are generally different. Thus, in the first (concentration dominant) part of the reactor at low frequencies, the temperature phase falls off at a rate that is intermediate between its behavior in an empty tube reactor and a nonreactive packed bed. When the temperature becomes dominant in the last part of the reactor at low frequencies, the temperature phase behaves almost as the phase of the heat regenerator [Equation (25)].

At moderate frequencies ($\omega \cong 7$), the phase of the temperature wave near the end of the reactor approaches a value that differs by π radians from the concentration phase. Since the concentration disturbance dominates at these conditions, such a phase relationship is untenable and is rapidly altered through the influence of concentration on the rate of heat generation to nearly either 2π or zero. The abrupt jump of the phase relationship from 2π to zero with a small increase in frequency is a manifestation of the phase discontinuity discussed earlier and is treated still further in a succeeding paragraph. Further, this aspect of the phase behavior is sensitive to the value of the ratio $(r_A + \gamma r_B)/H$. One can expect the behavior shown in Figure 6 when values of this ratio are of order unity. For small values of the ratio, the thermal dynamics dominate; the influence of the chemical reaction, while still evident, is much weaker.

As the frequency is increased further, the temperature phase approaches the concentration phase because the influence of the packing on the phase of thermal waves in packed beds diminishes with increasing frequency [Equation (25)]. Since concentration is dominant everywhere at high frequencies, one may therefore expect no extraordinary behavior of the temperature phase.

Temperature Forcing. PHASE OF TEMPERATURE. Because

the magnitude of the temperature wave dominates throughout the reactor up through the frequency 15.17 (see Figure 7), the phase of this wave is close to that of the nonreactive heat regenerator. The concentration wave, which lags behind the temperature wave, does exert some influence, however, and as a consequence, the phase of the temperature wave falls off somewhat more rapidly than that of the regenerator.

At the frequency 21.06, the magnitude of the concentration wave dominates near the end of the bed (this is not discernible in the graph) and induces, as discussed earlier, a rapid change in the temperature phase when the phase difference between temperature and concentration approaches π radians.

PHASE OF CONCENTRATION. The dominance of temperature at low frequencies forces the concentration wave to propagate at a rate nearly that of the temperature wave. The propagation rate, however, is somewhat faster than the temperature wave owing to the convection of reactant through the slowly moving temperature wave. As the frequency is increased, the phase of the concentration and temperature waves approach each other (ω = 14.32 and 15.17 of Figure 7) in a region of the reactor still dominated by the temperature wave. As discussed earlier, a zero phase relation in such circumstances is untenable, and the phase of concentration is altered rapidly to a value nearly π radians different from that of the temperature wave. The rapid phase change at these frequencies is first negative and then positive and is similar in many respects to the behavior of the temperature phase under concentration forcing shown in Figure 6.

At still higher frequencies (ω = 21.06), the concentration wave becomes dominant in the last 60% of the bed. An equivalence of phases of the temperature and concentration waves can therefore occur in this region without the abrupt change of phase observed at lower frequencies. In this region of the reactor, the concentration phase behaves nearly as $-\omega z$, essentially uninfluenced by the reaction.

An alternate graphical representation of the phase and amplitude behavior that is helpful in explaining the peculiarities of the phase is shown in Figure 8. Graphed here at selected frequencies are the loci of vectors whose magnitude and angle represent the amplitude and phase of the traveling waves of concentration and temperature. The parameter along the loci is position in the reactor.

Interest in these loci, which here pertain to the case of concentration forcing, centers on the behavior of concentration at low frequency and the behavior of temperature at higher frequencies. As is shown here and as observed earlier, the concentration wave at low frequencies is strongly influenced by the temperature wave in the latter half of the bed. Figure 8*a* illustrates the evolution of the positive phase relationship for reactant *A*. Thus, in the limiting case of zero frequency, the phase for reactant *A* is $+\pi$ in the latter part of the reactor and zero in the first part of the reactor. The point at which this switch in phase occurs has been termed the *concentration node point* (3, 4).

The behavior of the temperature locus at the two closely spaced frequencies shown in parts (*c*) and (*d*) of Figure 8 shows the origin of the phase discontinuity observed earlier. As discussed in connection with Figure 6, the dominance of the concentration wave strongly affects the temperature wave when the phase relation between them approaches π. Figures 8*c* and 8*d* show that the slight change in that interaction with increasing frequency causes the temperature locus to sweep past different sides of the origin. As a consequence, the temperature vector in passing through the bed at the higher frequency circumscribes the origin once less than it did at the lower frequency. A similar behavior is observed for the concentration vector under temperature forcing.

The difference in phase between component *A* and component *B* displayed in Figures 8*a* and 8*b* occurs only when the feed concentration is the forced variable and is explained as follows. The component conservation Equations (9) and (10) combine to give

$$\left(\frac{\partial}{\partial\tau}+\frac{\partial}{\partial z}\right)(b-\gamma a)=0 \tag{26}$$

which has a general solution

$$b(\tau,z)-\gamma a(\tau,z)=c^0(\tau-z) \tag{27}$$

where the function c^0 is determined from the boundary conditions at $z = 0$. When the feed concentration of component *A* is forced sinusoidally

$$a(\tau,0)=M_A{}^0\sin\omega\tau$$

Then, by (27)

$$c^0(\tau)=-\gamma M_A{}^0\sin\omega\tau$$

and

$$b(\tau,z)=\gamma M_A(\omega,\tau)\sin[\omega\tau+\varphi_A(\omega,z)]-\gamma M_A{}^0\sin(\omega\tau-\omega z) \tag{28}$$

Equation (28) states that the vector **b** consists of two components, one component traveling in phase with the vector **a** and varying in proportion to it and a second component of constant amplitude traveling with a phase angle of $-\pi$ plus the transport phase lag ωz. The phase difference between the vectors **a** and **b** will be zero, however, in the following three cases:

1. Feed concentrations of reactants *A* and *B* varied simultaneously such that $c^0(\tau) \equiv 0$.
2. Disturbance in temperature or velocity. In this case, the amplitude of the vector **b** is $\gamma M_A(\omega,\tau)$.
3. Stationary capacity for heat absent, in which case disturbances are in phase (or 180 deg. different) and propagate with the fluid velocity.

Amplitude Behavior

Because a crest in the temperature wave does not always coincide with a crest in the concentration wave, comparisons of only the amplitudes of concentration and temperature are of no assistance in interpreting the influence of one upon the other. Rather, to interpret the evolution of the amplitude of the concentration wave of component *A*, for example, the temperature encountered at each point in the bed by a crest in concentration must be known. For this example, the temperature encountered by the traveling concentration crest is simply the projection $\mathbf{p}_T$ of the temperature vector **t** upon the concentration vector **a**, which is

$$\mathbf{p}_T=M_T(\omega,z)\cos[\varphi_A(\omega,z)-\varphi_T(\omega,z)]\cdot\mathbf{a}/M_A$$

Two conditions may be distinguished here. When the phase difference $\Delta\varphi \equiv |\varphi_A - \varphi_T|$ lies in the interval $(4n-1)\,\pi/2 < \Delta\varphi < (4n+1)\,\pi/2$, both **a** and $\mathbf{p}_T$ have the same sense; this means that the temperature at the crest of the concentration wave acts in concert with concentration to increase the rate of chemical reaction. For such conditions, the temperature and the concentration waves may be said to interact or interfere constructively. The waves interfere destructively when $(4n+1)\,\pi/2 < \Delta\varphi < (4n+3)\,\pi/2$ because **a** and $\mathbf{p}_T$ then have opposing effects on the reaction rate. To assist in the interpretation of the amplitude behavior, regions of con-

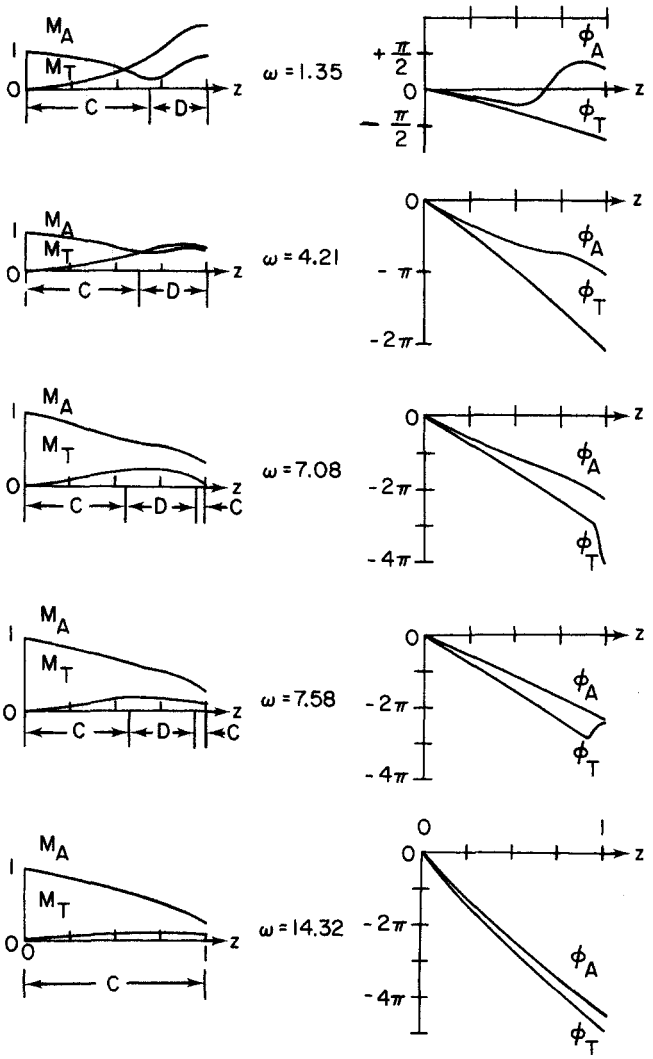

Fig. 6. Spatial variations in amplitude and phase at selected frequencies for sinusoidal forcing of the feed concentration of reactant A only: conditions of column 2, Table 2.

stuctive and destructive interference are indicated by *C* and *D*, respectively, on Figures 6 and 7.

Concentration Forcing (Figure 6). The most interesting behavior occurs at low frequencies; for example, $\omega = 1.35$. Since the early portion of the bed is a region of constructive interference, the concentration falls off at a rate faster than it would were there no influence of temperature. The rate of falloff slackens as the concentration wave passes through the region near the *C-D* transition because the influence of the temperature there is minimal ($\Delta\varphi$ is near $\pi/2$). In the constructive region, the induced temperature wave grows because the sensitivity functions r_A and r_T both increase with distance. For the same reason the temperature wave continues to grow even in the destructive region, becomes dominant there, and as a consequence of its inverted influence on the concentration in that region, it induces an increase in the amplitude of the concentration wave. The influence of destructive interference slows the rate of growth of both waves near the end of the bed where the phase difference is nearly 180 deg.

As frequency is increased, the pattern described above is altered owing principally to the increased attenuation of the thermal wave through heat transfer to the packing. For example, at $\omega = 7.08$, the temperature wave increases more slowly and never achieves dominance. In the region of constructive interference, therefore, the amplitude of the concentration wave falls off more slowly. In the destructive region, the amplitude of the temperature wave decreases owing to destructive interference. At the very end of the reactor there is a slight increase in the rate of falloff of the concentration amplitude owing to the constructive interference there. The pattern of interaction changes little as frequency is increased further.

The regions of constructive and destructive interference shown in Figure 6 pertain to the interference between the temperature and reactant *A* only. Since the phase of the wave of concentration of reactant *B* differs from that of reactant *A* and that of the temperature, interference among the three waves must be considered, with the result that regions of constructive and destructive interference cannot be defined unambiguously in all instances. For the case at hand, however, the influence of the wave of reactant *B* on the reaction rate was small because reactant *B* was in excess; for purposes of discussion of

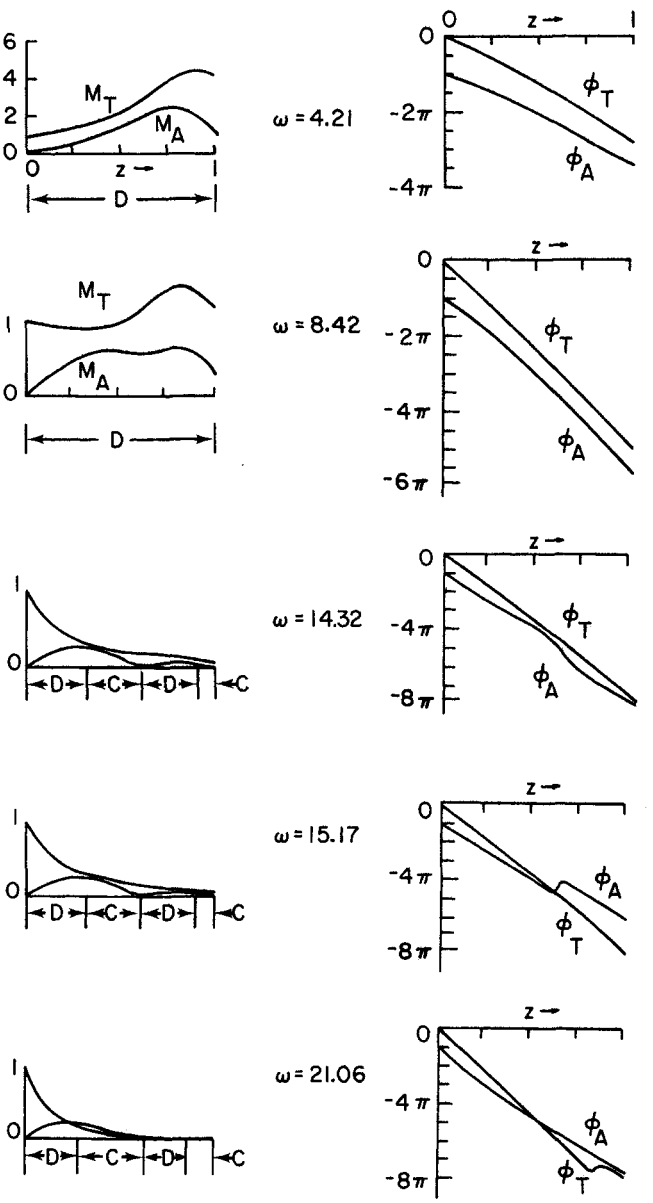

Fig. 7. Spatial variations in amplitude and phase at selected frequencies for sinusoidal forcing of the feed temperature: conditions of column 1, Table 2.

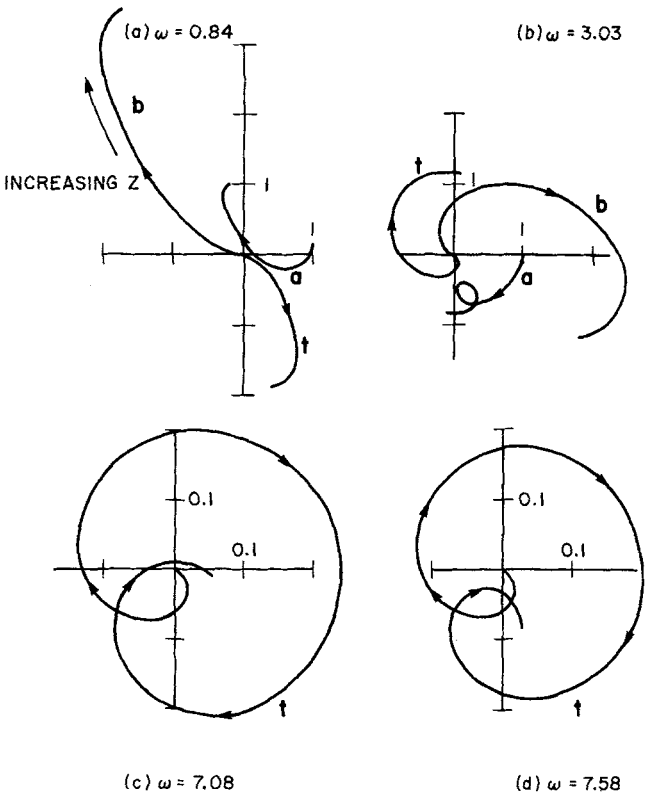

Fig. 8. Loci of the concentration and temperature vectors for forcing of the feed concentration of reactant A only: conditions of column 2, Table 2.

the interference phenomenon, its effect could be disregarded without consequence.

Temperature Forcing (Figure 7). While the amplitude behavior here differs in detail from that of the case of concentration forcing, the interference phenomenon, nevertheless, exerts similar influences on each variable. For example, at low frequency (say $\omega = 4.21$), the entire bed comprises a region of destructive interference; as a consequence, the temperature wave grows at a rate somewhat less than it would were there no concentration variations. The induced concentration wave grows primarily because the sensitivity of the reaction rate r_T grows with distance. Near the end of the bed, however, the destructive effect of the concentration becomes so large (because r_A becomes large) that both concentration and temperature amplitudes decline.

With increasing frequency, the increased attenuation of the temperature wave has an effect similar to that observed in the case of concentration forcing. The smaller temperature wave, attenuated owing to the finite rate of heat transfer between fluid and packing, induces smaller concentration waves. The influence of destructive interference on the concentration is seen again in the early portion of the bed. A region of constructive interference helps to delay the extinction of the concentration wave and retards also the decay of the temperature wave. These effects are small, however, in comparison with the destructive effects observed at low frequencies.

CONCLUDING REMARKS

These experiments have shown that a simple, one-dimensional model with distributed thermal capacitance may be used to represent the primary dynamic characteristics of a fixed bed reactor with liquid reactants. That such a simple model is applicable to such a complex process derives chiefly from the dominance of the thermal wave over other phenomena. One of the requisites for an accurate model of the reactor, therefore, is an accurate accounting of the rate of transfer of heat between the fluid and the stationary thermal masses and the storage of heat in those masses. These factors assume an importance comparable to that of the rate of heat generation and the rate of heat transfer to the external environment.

Factors of secondary importance in the present case appear to be axial fluid mixing, axial heat conduction, radial nonuniformities within the bed, and nonuniformity of temperature within the particles. All of these phenomena contribute to the axial dispersion of heat, but their influence is completely overshadowed by the dispersion caused by the finite rate of heat transfer between the fluid and the stationary thermal capacitance (3). Of secondary importance also is the influence of the nonlinearities of the reaction rate when the excursions about an operating point are modest. In the present case, a model incorporating a local linearization about an operating condition is clearly adequate for excursions in concentration as large as ± 10% and in temperature as large as ± 5°C. A model capable of representing process excursions of this magnitude would seem to be of value in studies of reactor control.

The computational study of disturbance propagation has revealed several aspects of dynamical behavior that are peculiar to reactors of this type. The remarkable behavior of the phase relation between the temperature and concentration waves, the phase discontinuity, and the interference phenomenon all seem to imbue the fixed bed reactor with a special character seldom found in other chemical processes. The genesis of these unique dynamical characteristics may be identified with the strong coupling between two or more traveling disturbances, a difference in speed of propagation of these disturbances, and the variation of the rate of chemical reaction throughout the reactor. These conclusions regarding the nature of wave propagation are based on a locally linearized model of the reactor but are believed to remain valid in most instances, even in the presence of nonlinear effects. For example, a nonlinear computational analysis (3) of transients in this reactor did not reveal any extraordinary behavior due to nonlinear effects. In this case, the influence of the nonlinear phenomena appears to be far less significant than the influence of the nonuniformity of the reaction rate sensitivity throughout the reactor. In catalytic reactors, however, the nonlinear effects must be given closer examination; there, the stability of the catalyst particles may be of paramount importance.

ACKNOWLEDGMENT

The authors gratefully acknowledge the support of this work by the National Science Foundation.

NOTATION

a = disturbance in concentration of reactant A, $A - A_s$
a = two-dimensional vector whose magnitude and angle represent the amplitude and phase of the reactant A concentration wave
$\bar{a}$ = Laplace transformation of a
a_p = surface area of particles per unit volume of bed
A = dimensionless concentration of reactant A, A^*/A_r
A^* = concentration of reactant A, sodium thiosulfate

A_r = constant reference concentration of reactant A that is representative of the feed concentration; for example, if the feed concentration varies sinusoidally, A_r is its average value

A_s = dimensionless concentration of reactant A in the reactor at steady state

$\mathcal{A}$ = dimensionless Arrhenius parameter, E/RT_r

B = dimensionless concentration of reactant B, B^*/A_r

B^* = concentration of hydrogen peroxide

$b, \mathbf{b}, \bar{b}, B^*, B_s$ = concentration variables for reactant B, hydrogen peroxide; definitions similar to those for reactant A

c_f = heat capacity of the fluid

c_p = heat capacity of the particles

c_w = heat capacity of the tube wall

D_i = inside diameter of tube wall

D_o = outside diameter of tube wall

D_p = diameter of particles

E = activation energy of the reaction

G = mass flow rate based on superficial cross-sectional area of tube

h_e = external environment-wall heat transfer coefficient

h_p = particle-fluid heat transfer coefficient

h_w = wall-fluid heat transfer coefficient

H = compound heat transfer parameter used in simplified model, related to individual heat transfer parameters by Equation (19)

H_e, H_p, H_w = dimensionless heat transfer parameters: $h_e 4L/\epsilon D_o V_r \rho_f c_f$, $h_p a_p L/\epsilon V_r \rho_f c_f$, and $h_w 4L/\epsilon D_i V_r \rho_f c_f$, respectively

i = imaginary unit, $\sqrt{-1}$

k = reaction rate constant

K = dimensionless reaction rate parameter, $kA_r(L/v_r)\exp(-\mathcal{A})$

L = length of packed bed

m_w = mass of tube wall per unit volume of packed bed

M_i = amplitude of the sinusoid of variable i; M_i^0 denotes the amplitude at $z = 0$

$\mathbf{p}_T$ = projection of the temperature vector $\mathbf{t}$ onto the vector $\mathbf{a}$

R = universal gas constant

r = dimensionless reaction rate, $KAB \exp\{\mathcal{A}T/(T_0 + T)\}$

r_A = sensitivity of reaction rate to the concentration of reactant A, $\partial r_s/\partial A_s$

r_B = sensitivity of reaction rate to the concentration of reactant B, $\partial r_s/\partial B_s$

r_s = dimensionless reaction rate under steady state conditions

r_T = sensitivity of reaction rate to temperature, $\partial r_s/\partial T_s$

s = complex variable

t = disturbance in fluid temperature, $T - T_s$

$\mathbf{t}$ = fluid temperature vector analogous to the vector $\mathbf{a}$

$\bar{t}, \bar{t}_e$ = Laplace transformation of t and t_e

t_m = temperature of solid media in the simplified model

t_p, t_w, t_e = disturbances in the temperature of the particles, tube wall, and external environment, $T_p - T_s$, $T_w - T_{ws}$, and $T_e - T_{es}$, respectively

T = dimensionless temperature of the fluid, $(T^* - T_r)/\Delta T_a$

T_p, T_w, T_e = dimensionless temperature of the particles, tube wall, and external environment, $(T_p^* - T_r)/\Delta T_a$, $(T_w^* - T_r)/\Delta T_a$, and $(T_e^* - T_r)/\Delta T_a$, respectively

T^* = temperature of the fluid

T_p^*, T_w^*, T_e^* = temperature of the particles, tube wall, and external environment

T_0 = dimensionless parameter, $T_r/\Delta T_a$

T_r = constant reference temperature that is representative of the feed temperature

T_s = dimensionless fluid temperature at steady state

T_s' = axial temperature gradient at steady state, dT_s/dz

U = dimensionless overall heat transfer coefficient, $H_w H_e/(H_w + H_e)$

v = disturbance in fluid velocity, $V - 1$

$\bar{v}$ = Laplace transformation of v

V = dimensionless fluid velocity, V^*/V_r

V^* = interstitial fluid velocity

V_r = constant reference fluid velocity taken as the time average of V^*

z = dimensionless distance, z^*/L

z^* = distance from the inlet of the reactor

Greek Letters

β_p, β_w = dimensionless thermal capacity ratios, $\dfrac{\epsilon\rho_f c_f}{(1-\epsilon)\rho_p c_p}, \dfrac{\epsilon\rho_f c_f}{m_w c_w}$

β = compound thermal capacity ratio used in simplified model

γ = stoichiometric coefficient for the chemical reaction

$(-\Delta H)$ = heat of reaction

ΔT_a = adiabatic temperature rise, $(-\Delta H)A_r/\rho_f c_f$

$\Delta\varphi$ = absolute value of the phase difference $\varphi_A - \varphi_T$

ϵ = void fraction of the packed bed

μ = fluid viscosity evaluated at a mean reactor temperature

ρ_f, ρ_p = density of fluid and particles, respectively

τ = dimensionless time, $\tau^* V_r/L$

τ^* = dimensional time

φ_A, φ_T = phase of reactant A and temperature relative to phase of forced variable at reactor inlet

ω = dimensionless frequency, $\omega^* L/V_r$

ω^* = dimensional frequency, radians/unit time

LITERATURE CITED

1. Cairns, E. J., and J. M. Prausnitz, *Ind. Eng. Chem.*, **51**, No. 12, 1441 (1959).
2. Cohen, W. C., and E. F. Johnson, *Chem. Eng. Progr. Symposium Ser. No. 36*, **57**, 86 (1961).
3. Crider, J. E., and A. S. Foss, *AIChE J.*, **12**, 514 (1966).
4. *Ibid.*, **14**, 77 (1968).
5. Liu, Shean-Lin, and N. R. Amundson, *Ind. Eng. Chem. Fundamentals*, **1**, 200 (1962); **2**, 12, 183 (1963).
6. McGuire, M. L., and Leon Lapidus, *AIChE J.*, **11**, 85 (1965).
7. Meek, R. M. G., "International Developments in Heat Transfer," Pt. 4, p. 770, Am. Soc. Mech. Engrs., New York (1961).
8. Penrod, D. D., and E. D. Crandall, *Ind. Eng. Chem. Fundamentals*, **5**, 581 (1966).
9. Petersen, E. E., "Chemical Reaction Analysis," p. 244, Prentice-Hall, Englewood Cliffs, N. J. (1965).
10. Schwartz, C. E., and J. M. Smith, *Ind. Eng. Chem.*, **45**, 1209 (1953).
11. Spencer, J. L., Ph.D. thesis, Univ. Pa., Philadelphia (1961).
12. Tinkler, J. D., and D. E. Lamb, *Chem. Eng. Progr. Symposium Ser., No. 55*, **61**, 155 (1965).
13. Deans, H. A., and Leon Lapidus, *AIChE J.*, **6**, 663 (1960).

Manuscript received July 10, 1968; revision received November 13, 1968; paper accepted November 14, 1968. Paper presented at AIChE Philadelphia meeting.